AIS Assisted Identification and Refocussing of Ships in Airborne SAR Images

Scheiber, Rolf, German Aerospace Center (DLR), rolf.scheiber@dlr.de, Germany
van Kempen, Michel, German Aerospace Center (DLR), michel.kempen@dlr.de, Germany

Abstract

The Automatic Identification System (AIS) was established as a cooperative system for maritime surveillance, collision avoidance and combating illegal fishery. However, violations of AIS regulations need to be identified by independent sensors. This paper investigates possibilities for joint evaluation of AIS signals and simultaneously acquired high resolution airborne SAR images with respect to vessel identification and AIS signal integrity. For this purpose DLR's F-SAR system collected data at the North Sea coast. The AIS data at the time of overflight were used to identify, precisely locate and refocus the vessels in the SAR image.

1 Introduction

International regulations require ships above certain gross tonnage and all passenger ships to broadcast their AIS signal at all times, except where international agreements, rules or standards provide for the protection of navigational information [1]. Smaller vessels are excluded from this regulation and often there are cases where the AIS signals are manipulated or switched off, in order to camouflage forbidden activities like illegal fishery or fuel dumping. In this sense the available AIS signals are termed incomplete and not fully reliable. On the other side, SAR imaging can provide high resolution maps of a pretty large maritime area, independent of weather conditions and daylight. Although individual vessels can be detected by automatic means, their identification is very challenging without external information. Thus, AIS signals and SAR images provide complementary information and their synergy is important for improving the integrity and completeness of data for maritime surveillance.

AIS signals are broadcast at VHF freuencies. AIS derives the position and timing information from GPS, including a differential GNSS receiver for precise position in coastal and inland waters. Other information may be obtained from shipboard equipment through standard marine data connections. Heading information and course and speed over ground is normally provided by all AIS-equipped ships. Usually, the updates are transmitted at irregular intervals of 30 seconds to several minutes, depending on geographic position and density of traffic, taking into account the limitations of the VHF channel.

Routine SAR imaging is presently possible only at few time instants depending on satellite overpasses. A flexible way to locally improve the surveilance rate is by deploying airborne SAR sensors. They allows imaging at sub-meter resolution scale, covering a swath width of 1-10km, depending on operating altitude. In spaceborne SAR images, travelling vessels are only sligthly defocused, but the situation is different in the airborne case. Defocussing is certain due to the much lower aircraft speed and larger integration times. In addition, there is always the azimuth mis-location problem in case of across-track velocity components.

For investigating the benefits of synergistic use of AIS signals and airborne SAR data, DLR has conducted a first measurement campaign in June 2016 at the North Sea coast using its F-SAR airborne sensor [2].

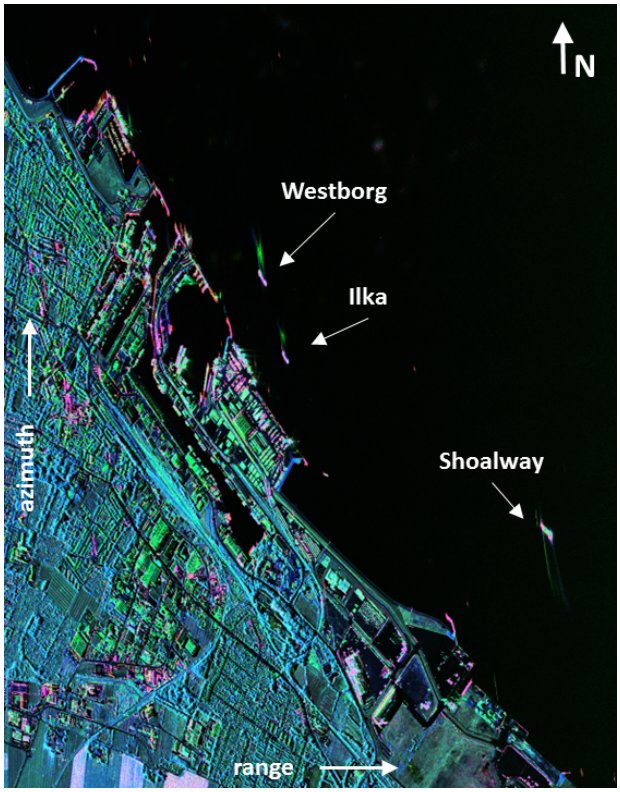

Figure 1: F-SAR image of Cuxhaven harbour, acquired on 28-Jun-2016, 14:36:39 (UTC) , X-band polarimetric Pauli representation (RGB: HH-VV, 2HV, HH+VV). Identification of 3 ships based on their AIS data.

ISBN 978-3-8007-4636-1 / ISSN 2197-4403

Dual-frequency, X- and L-band polarimetric data were acquired from an altitude of 5600m along different flight tracks in the coastal area of Cuxhaven, an area of highly frequented shipping routes. The data were used to develop an automatic identification, localisation and refocusing module for ships with co-located AIS data during SAR data acquisition. Section 2 discusses the need for a filtering operation to exclude AIS signals not relevant for the time interval and imaged area of the SAR acquition, followed by the localisation operation in SAR coordinates. Using the computed range/azimuth position in the image, different refocusing operations are performed on the vessel's image patch, as discussed in section 4. The refocusing kernel uses the along- and across track velocities computed from the AIS signal, optionally followed by an autofocus procedure. A result of vessel refocusing is shown in section 4, followed by a discussion on limitations of the method in section 5, which also concludes the paper.

2 Localisation based on AIS data

Figure 1 shows the harbour area of Cuxhaven as imaged by the F-SAR sensor. Most of the vessels anchor in the harbour, but three travelling ships can easily be recognized. For maritime surveillance it is essential to find the correspondance of AIS signals to vessels imaged by the airborne SAR sensor. For correct and unambiguous localisation the bunch of AIS signals undergoes a threefold filtering operation:

- by time: Each vessel's AIS signal is resampled to the time vector of the SAR acquisition. AIS signals outside the SAR time interval are excluded from further analysis.
- by location: The distance vector d as a function of time t is computed. All distances outside the radar's receive window are excluded, as the corresponding ships are not imaged by the radar. In addition, the radar viewing direction - F-SAR is right looking - is taken into account to exclude vessels from the opposite side.
- by Doppler frequency: Each AIS signal is limited to the time interval it is imaged by the antenna pattern, corresponding to the operated pulse reptiion frequency PRF (or more restrictive to the processed Doppler bandwidth):

$$|\frac{2}{\lambda}\frac{\delta d}{\delta t} - f_{dc}| < \frac{PRF}{2}. \quad (1)$$

The range histories of the vessels passing these threefold filter are then used to determine their positions in the slant range radar image. Usually, the positions correspond to the zero-Doppler time, i.e. the azimuth and range position, where the derivative of the range history is zero. However, in case of squinted acquisitions this approach is not sufficiently reliable. In that case, the last AIS filtering operation needs to account for the Doppler centroid f_{dc} and the range/azimuth positions need to be estimated in beam center geometry. Otherwise, some of the imaged vessels might be missed, especially if they are located at the image borders.

Vessel	θ[deg]	v_{az}[m/s]	v_{rg}[m/s]	r[km]
ILKA	138.8	-3.771	3.265	8.4
WESTBORG	140.3	-5.584	4.594	8.3
SHOALWAY	306.4	2.694	-3.218	9.9

Table 1: Relevant vessel properties at the time of SAR imaging.

Knowing the course of the vessel θ, its distance to the radar, as well as the SAR sensor's track angle, it is possible to compute the velocity components in azimuth v_{az} and slant-range v_{rg} projection, needed for the parametric refocusing operation to be discussed in section 3.1. The AIS-derived parameters of the three moving vessels in **Figure 1** are summarized in **Table 1**.

3 Refocusing based on AIS data

Refocusing of each vessel is essentially performed by a 2D parameteric approach. For additional precision and/or confirmation of AIS-derived velocity parameters an additional autofocus is suggested. For each vessel passing the three-fold filtering operation, a patch of single-look complex SAR data is extracted. It's dimensions depend on both, the vessel size and its velocity parameters. It is important to ensure that the patch covers the real (averaged) position during SAR illumination and the one the vessel is imaged to during the SAR processing. Otherwise the output of the refocussing operation becomes backfolded due to the potentially large cross-track velocity component.

3.1 Parameteric 2D refocusing

The parametric refocussing uses the SAR raw signal description in 2D frequency domain (i.e. impulse response function), computed for the range r_0 corresponding to the distance of closest approach, as computed from the AIS data. The sequence of operations is shown in **Figure 2**.

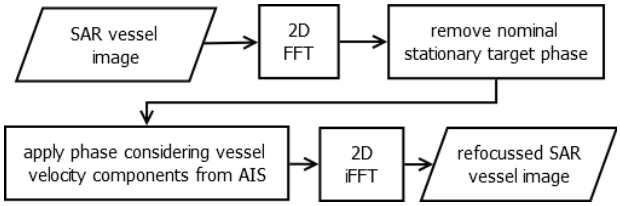

Figure 2: Block diagram of the parametric refocusing.

The derivation is performed using te principle of stationary phase in a similar way as in [3] for calculating the spectrum of a stationary target at slant range r_0, however

introducing in addition the cross-track and along-track velocity components, v_{rg} and v_{az} in the starting equation for the range history. Using parabolic approximations, the 2D spectrum can be described as a function of range and azimuth frequency, f_τ and f_η:

$$\Phi_{MT}(f_\tau, f_\eta) = -\frac{2\pi}{a(f_\tau)} \cdot (r_0 - \frac{b^2}{2c}) + \frac{2\pi b}{c} f_\eta + \frac{\pi a(f_\tau)}{c} f_\eta^2, \quad (2)$$

with $1/a(f_\tau) = 2(1 + \frac{f_\tau \lambda}{c_0})/\lambda$, $b = v_{rg}/sin^2(\theta_{inc})$, and $c = (v - v_{az})^2/r0$. For $v_{az} = v_{rg} = 0$ we obtain $b = 0$ and $c = v^2/r_0$ and the above equation reduces to:

$$\Phi_{ST}(f_\tau, f_\eta) = -\frac{2\pi}{a(f_\tau)} \cdot r_0 + \frac{\pi a(f_\tau)}{c} f_\eta^2. \quad (3)$$

Eq. 3 removes the nominal stationary target phase, whereas eq.2 computes the matched phase to the vessel's velocity components. This method ideally removes the defocusing in azimuth and (!) slant-range directions and also shifts the refocused vessel to its nominal position.

3.2 Refocusing with PGA-autofocus

As AIS signals might not be sufficiently accurate for optimum focusing, the phase-gradient autofocus (PGA) algorithm is applied in addition [4]. It is able to estimate also higher order phase errors as might originate from ocean swell, and is particularly useful for smaller size vessels.

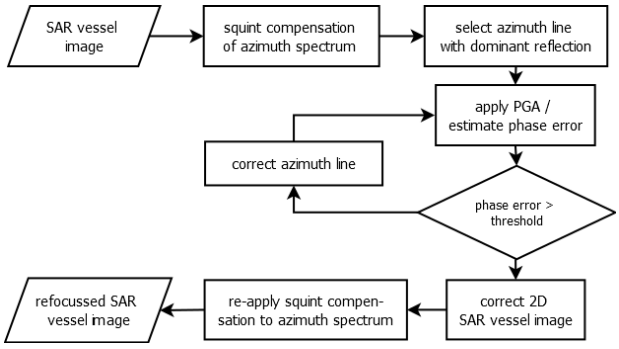

Figure 3: Block diagram of the refocusing based on PGA autofocus.

In a first implementation, only one dominant reflection (a single azimuth line) is used for iterative PGA estimates and the result is applied to the whole patch (see **Figure 3**). Opposite to the original PGA taylored to Spotlight SAR data, which result in an image in azimuth frequency domain, our implementation starts with an azimuth line in time domain, which is windowed for the dominant reflection, and transformed to the frequency domain, g_w. In consequence, the PGA operation is applied with the azimuth frequency f_η as argument:

$$\dot{\phi}_e(f_\eta) = \frac{\mathrm{Im}[\dot{g}_w(f_\eta) g_w^*(f_\eta)]}{|g_w(f_\eta)|^2} \quad (4)$$

The estimated phase error derivative $\dot{\phi}_e$ is integrated and used to correct the azimuth spectrum. After iFFT the focused vessel is used to find the dominant point for the next iteration (for convergence reasons preferably within the same azimuth line).

3.3 Quality measure

We consider the intensity-squared metric to provide a quantitative measure of image sharpness, defined as the sum of all squared pixel intensities I within one vessel image patch [6].

$$S = \sum_{az} \sum_{rg} |I(rg, az)|^2 \quad (5)$$

For each refocusing attempt we compute the image sharpness factor as the ratio of refocused vs. original, stationary focused image sharpness: $shf = \frac{S_{refoc}}{S_{input}}$. The higher the shf the better the focussing.

4 Results

The vessel *WESTBORG* (see **Figure 4**) was selected to demonstrate the achievable re-location and re-focusing performance. The pictures in **Figure 5** are obtained after nominal SAR focusing and after several refocusing operations. The vessel travels with considerable velocity components in azimuth and range. It is thus defocussed and displaced from its real geographic position (projected in slant range), which is marked by the red X. When only the range velocity component is corrected, the ship is re-displaced to its expected position, but stays defocussed (not shown). The 2D parametric refocussing corrects both effects, such that the ship appears focussed and at its expected position (*shf=23.4*). Further, some details of the ship's superstructural parts can be identified. When refocussing is performed solely by means of autofocus, the defocusing can be corrected only to a certain extend (*shf=2.1*), unless the autofocus result is used to estimate the along-track velocity to serve as a parametric input to the 2D correction of section 3.1. Also the mis-location is still there, similar to the case when only the azimuth velocity component is used for parametric refocusing (not shown). The best result is obtained when the result of the 2D parametric focusing is ammended by a residual autofocus operation. This leads to the highest sharpness factor (*shf=23.9*) and the autofocus phase estimate can be used to confirm the vessel's azimuth velocity component derived from the AIS annotation (in this case a very good match). Having the ship properly focussed, it is possible to estimate its length with few meter accuracy, enabling its categorisation and even its travel direction. The estimated ship length is 85m, whereas the annotation in the AIS data is 89m. Any mismatch with AIS data can be used to flag the detection as not reliable or the AIS data as doubtful.

ISBN 978-3-8007-4636-1 / ISSN 2197-4403

Figure 4: General Cargo Ship *WESTBORG* [5]. During data acquisition it's AIS signal indicated a speed of $7.2m/s$ at a course of 140^o.

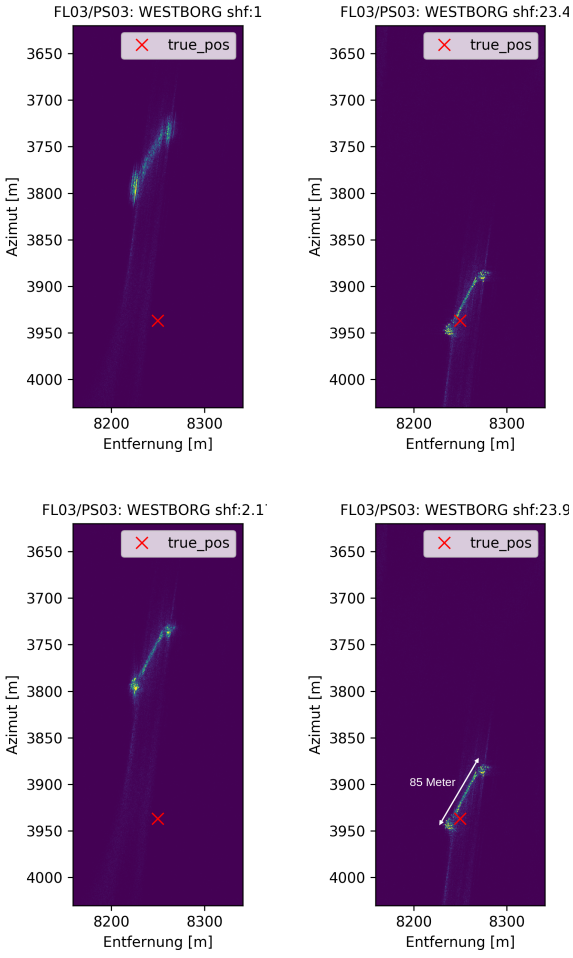

Figure 5: Vessel *WESTBORG*: (top left) defocssed and displaced signal after nominal SAR focusing; (top right) after parametric 2D refocussing; (bottom left) after 1D PGA autofocus and (bottom right) after parametric refocussing followed by 1D autofocus. Right looking aircraft heading was towards north (i.e. image bottom).

5 Conclusions

The analysis performed in this paper indicate the feasibility of precise location and refocusing of vessels in single channel airborne SAR images based on their AIS signals. The autofocus operation allows to confirm the azimuth component of the vessels' speed, whereas the refocused pattern allows to check for the ships' course and its dimensions. Thus the integrity of the received AIS signals can be verified to a certain amount. In the absence of AIS signals, the analysis also show that the autofocus algorithm is able to perform precise focusing. In that case only the azimuth velocity component is estimated with high precission, whereas the range component needs to be inferred - with some ambiguity - from the vessels' orientation. Unambiguous and precise (or accurate) estimation of vessels' speed and actual geographical location is only possible with multi-channel SAR systems [7]. For demonstrating the (near) real-time performance of airborne SAR for maritime surveillance purposes, DLR's airborne SAR system is about to be interfaced with an onboard AIS receiver, such that results similarto those presented in this paper can be performed in future directly onboard the aircraft.

References

[1] International Maritime Organization: *http://www.imo.org/en/OurWork/safety/navigation/pages/ais.aspx*.

[2] St. V. Baumgartner, *Linear and Circular ISAR Imaging of Ships Using DLR's Airborne Sensor F-SAR* in Proceedings of International Conference on Radar Systems (IET Radar), Belfast, UK, October 2017.

[3] Cumming, I.G. and Wong, F.H.: *Digital Processing of Synthetic Aperture Radar Data: Algorithms and Implementation*, Artech House, pp., 2005.

[4] Carrara, W.G. and Goodman, R.S. and Majewski, R.M.: *Spotlight Synthetic Aperture Radar: Signal Processing Algorithms*, Artech House, pp. 264-268, 1995.

[5] Vessel Finder: *https://www.vesselfinder.com/ship-photos/203802?s=1*.

[6] Richard A. Muller and Andrew Buffington: *Real-time correction of atmospherically degraded telescope images through image sharpening*, J. Opt. Soc. Am., vol. 64, no. 9, pp. 1200-1210, Sept., 1974.

[7] S. V. Baumgartner and G. Krieger, *Multi-Channel SAR for Ground Moving Target Indication*, in Academic Press Library in Signal Processing: Communications and Radar Signal Processing, 1st ed., R. Chellappa and S. Theodoridis, Eds. UK ad USA: Academic Press (ELSEVIER), vol. 2, ch. 18, pp. 911-986, 2014.

ISBN 978-3-8007-4636-1 / ISSN 2197-4403